Communication: Combinatorial gradient techniques are used to map the morphology dependence of thin symmetric diblock copolymer films on film thickness and substrate surface energy. An inversion from symmetric to anti-symmetric lamellar morphology occurs with a progressive change in surface energy. An intermediate neutral region is found between these limiting types of ordering. The width ω of this transitional energy range scales as a power of copolymer mass M, $\omega \propto M^{1.9}$.

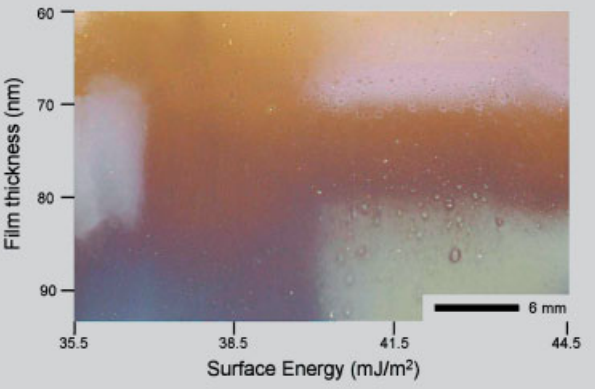

Optical photograph of a combinatorial map of the thin-film block-copolymer morphology on a film thickness and surface energy gradient. Island and holes on the surface scatter light causing the film to appear cloudy (lighter in color) in the areas where they exist. The darker areas do not have surface features and do not scatter light.

Combinatorial Mapping of Surface Energy Effects on Diblock Copolymer Thin Film Ordering

Archie P. Smith,[a] *Amit Sehgal, Jack F. Douglas, Alamgir Karim,* Eric J. Amis**

Polymers Division, National Institute of Standards and Technology, Gaithersburg, MD 20899, USA
E-mail: alamgir.karim@nist.gov

Keywords: block copolymers; combinatorial mapping; surface energy; thin films

Introduction

The self-organizational properties of block copolymers make them attractive for nanoscale applications that build on or exploit their molecularly tunable ordered morphologies.[1] These materials are also being increasingly utilized in traditional surfactant applications, such as compatibilizers, thickeners, emulsifying agents and adhesives. Recent work has shown that thin block copolymer films exhibit a surface pattern formation over a wide range of scales (nm to μm) that depend sensitively on film thickness,[2–4] temperature,[5,6] molecular weight,[7–11] and surface energy.[10,12–15] An understanding of this behavior is essential to the continuing use of these materials, but this multiparameter space is large for exploration using conventional techniques. This situation lends itself well to combinatorial investigation of the essential factors that control surface pattern formation.[3,4] The present study focuses specifically on the interplay between finite film thickness and surface energetics for morphological control of the patterns. Specifically, we introduce combinatorial continuous gradient methods (surface-energy thickness) for high-throughput determination of block copolymer surface morphology on a single test substrate.

Diblock copolymers are composed of two dissimilar polymers covalently linked at their ends.[16] As with many polymers, the individual blocks do not tend to mix well because of their low entropy of mixing, typically leading to microphase separation on cooling. When the two blocks have nearly the same polymerization index (''symmetric diblock copolymer''), a lamellar morphology is formed upon ordering. Previous work has shown that when these polymers are cast as thin films, a preferential surface interaction between one of the blocks and the substrate causes the lamellae to become oriented parallel to the substrate.[2,17–22] These films are smooth when the film thickness (h) is an integral multiple of the lamella thickness (L_o) but have an incomplete surface lamella that forms islands or holes of L_o when the thickness deviates from this value.[2–4] In addition to film thickness, the substrate surface energy (γ_s) may affect the morphology of the thin film.[12–15,23–27] When one block of the copolymer has an energetic preference for both the substrate and the polymer-air (''free'')

[a] Current address: Columbian Chemicals Company, 1800 West Oak Commons Ct., Marietta, GA 30062, USA.

  1022-1336/2003/0101–131$17.50+.50/0

surface, the values of the film thickness at which the film is smooth h_s is an integral multiple of the lamellar thickness ($h_s = m \cdot L_o$; m is an integer) and such films are termed ''symmetric''. The anti-symmetric boundary condition occurs when one block prefers the substrate and the other the free surface, leading to $h_s = (m + 1/2) \cdot L_o$. Somehow a crossover between the symmetric and anti-symmetric ordering must occur as the energetic preference for one block changes over to the other. This crossover clearly has implications for surface-pattern formation. It is unclear what role finite film thickness plays in this crossover. This motivates our combinatorial investigation into surface-pattern formation of the block copolymer using orthogonal gradients in h and γ_s.

Experimental Part

A simple method for chemical modification combining chlorosilane chemistry for covalent self-assembly of monolayers on silicon wafers and UV ozonolysis is used to generate stable gradient energy test substrates. The Si wafers (10 cm, n-type, ≈500 μm thick, ⟨100⟩ orientation, Wafer World Inc.[b]) were pre-cleaned and treated with UV/ozone plasma (Jelight UVO-Cleaner™, Model 42) for (15 to 20) min to remove organic contamination and form an oxide surface layer. The wafer was then placed in a solution of octyldimethylchlorosilane (>95% mass fraction, $\overline{M}_w = 206.83$,[c] Gelest Inc.) with a mass fraction of 2.5% in toluene for at least 45 min to form a self-assembled monolayer (SAM) at the substrate surface.[28] The substrate is thoroughly washed with toluene and dried, and the SAM is then exposed to a gradient of UV/ozone (UVO) radiation through a fused silica linear variable neutral density filter (gradient evaporated inconel, Maier Photonics, Inc.) or by accelerated exposure through a slit. In the UVO photooxidation the short-wavelength UV radiation (184.9 nm dissociates molecular oxygen, 253.7 nm dissociates ozone) produces atomic oxygen from air. A systematic change in optical density of the filter or the gradient in UV dosage directly translates into the progressive variation in the nominal concentration of ozone or atomic oxygen in close proximity of the surface. The graded oxidative process results in surface chemical modification by the generation of a gradient in surface chemical moieties (carboxyl, carbonyl and other oxygenated functionalities) across the sample.[26,28,29] The surface chemical signature was characterized by high-throughput time-of-flight secondary ion mass spectrometry (ToF-SIMS) spectra acquired in an automated fashion.[29] The change in surface energy induced by the addition of a surface functionality gradient is evaluated by static contact-angle measurements of water (θ_w) and diiodomethane ($\theta_{CH_2I_2}$) droplets with a Kruss G2 contact-angle measuring system. A representative set of these results is shown in Figure 1. Three images (Figure 1a–c) of water droplets from various locations on the substrate are shown along with a plot of θ_w vs position for the entire gradient (Figure 1d). The plot shows that θ_w varies linearly across the gradient. The surface energy (γ_s, also shown in Figure 1d) is estimated from the spatially resolved θ_w and $\theta_{CH_2I_2}$ contact-angle measurements using the Good and Girifalco geometric mean approximation (GMA) method.[29–32]

Thin films of near symmetric polystyrene-*block*-poly(methyl methacrylate) (PS-*b*-PMMA) diblock copolymers with three different molecular weights are cast onto these γ_s gradients. These materials were purchased from Polymer Source Inc. and were used as received. The molecular characteristics (as provided by the supplier) of each copolymer are given in Table 1. The unreacted homopolymer contamination is estimated to be less than 4% based on gel permeation chromatography (GPC) and nuclear magnetic resonance (NMR) data provided by the supplier. Thin films of the block copolymer with a gradient in thickness were cast on the gradient energy substrates from toluene solutions orthogonal to the γ_s gradient using the flow-coating method described previously.[3,4,33] The orthogonal gradients of film thickness and surface energy create an array of thousands of combinations of test conditions (state points) of film thickness and surface energy on a single substrate. For the experiments presented here, solutions of mass fraction 2% to 4% were used producing films with h ranging from 40 nm to 100 nm. Film

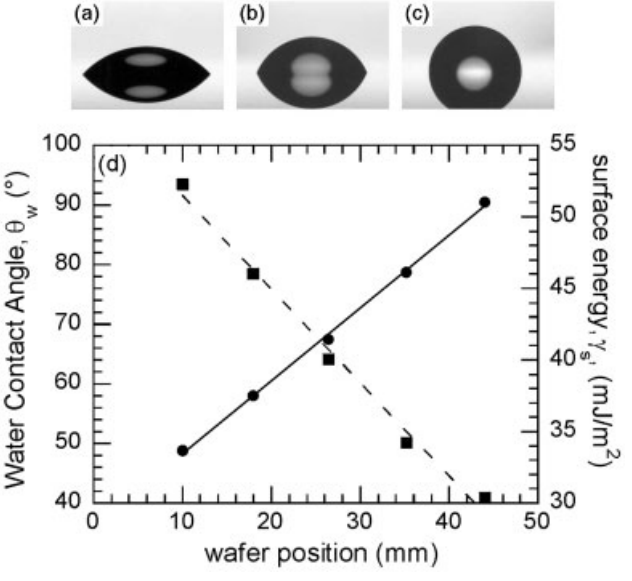

Figure 1. Photographs of water droplets at position (a) 10 mm, (b) 26 mm, and (c) 44 mm demonstrating the change in contact angle as a function of position. (d) Plot of water contact angle (solid line) and surface energy (dashed line) as a function of wafer position showing the linear change as a function of position.

[b] Certain equipment, instruments and materials are identified to adequately specify experimental details. Such identification does not imply recommendation by the National Institute of Standards and Technology.

[c] According to ISO 31-8, the term ''molecular weight'' has been replaced by ''relative molecular mass'', M_r. The conventional notation, rather than the ISO notation, has been employed for this publication.

Table 1. Molecular characteristics and derived neutral region widths for the molecular weights employed in this study. Errors given are the standard uncertainties.

Label	$\bar{M}_n$ S block	$\bar{M}_n$ MMA block	$\bar{M}_w/\bar{M}_n$	L_o[4]	ω, FWHM
	g/mol	g/mol		nm	mJ/m^2
26k	12 800	12 900	1.05	17.1	0.97 ± 0.16
51k	25 300	25 900	1.06	30.2	4.8 ± 0.6
104k	50 000	54 000	1.04	42.3	13.6 ± 2.1

thickness was characterized using an automated Filmetrics F20 UV-visible interferometer with 0.5 mm spot-size (with standard uncertainty ± 1 nm at 500 nm film thickness) every 2 mm across the gradient sample. Samples were subsequently annealed at 170 °C under vacuum for up to 96 h to allow ordering of the film. Contour maps of film thickness and the spatially resolved surface-energy measurements were used to generate the co-ordinate matrix of test locations for subsequent measurements. The surface patterns thus formed were then studied using automated atomic force microscopy (AFM, Digital Nanoscope Dimension 3100) along isoparametric lines at predetermined co-ordinates to determine the effect of γ_s and h on the surface pattern morphology of the block copolymer.

Results and Discussion

The block copolymer morphology generated with the combinatorial mapping is demonstrated in Figure 2, which shows an optical photograph of an $M = 51$k PS-*b*-PMMA copolymer thin film with both h and γ_s gradients. The h increases from top to bottom and varies between 60 nm to 95 nm, while γ_s increases from left to right and varies between 35.5 mJ/m^2 to 44.5 mJ/m^2. The lighter areas of the figure correspond to the formation of surface patterns

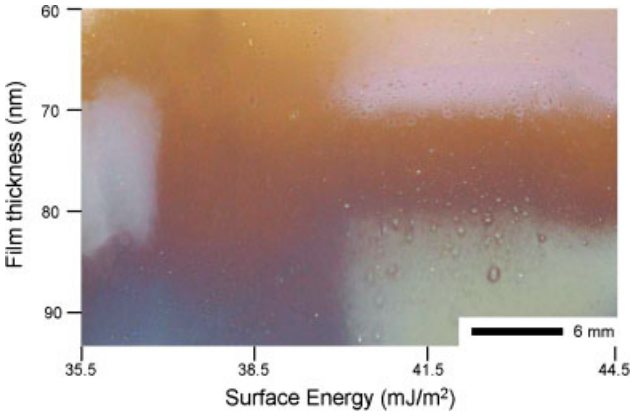

Figure 2. Optical photograph of a combinatorial map of the thin-film block-copolymer morphology on a film thickness and surface energy gradient. Island and holes on the surface scatter light causing the film to appear cloudy (lighter in color) in the areas where they exist. The darker areas do not have surface features and do not scatter light.

(islands and holes) which scatter visible light and make the film appear cloudy. Areas that appear dark are regions that have no surface features and are smooth such that they do not scatter light. The region near the left side of the photograph shows the morphology of the symmetric case, where the PS block is near the substrate and the free surface. Conversely, the right side of the photograph shows the morphology of the anti-symmetric case, where PMMA is at the substrate and PS is at the free interface. As expected, h_s is shifted by $L_o/2$ ($L_o = 30$ nm for this molecular mass polymer) when the block copolymer film changes from a symmetric to anti-symmetric morphology.

The dark region near the left center of the photograph, which exhibits no surface pattern formation for any h, corresponds to the "neutral" transitional surface energy region, γ_{sn}. It has been found previously[13–15,23,25,27] that for certain surface energies both blocks of the copolymer have a similar affinity for the substrate, i.e. the neutral substrate. In this case, the polymer chains orient parallel to the substrate surface such that the lamellae orient perpendicular to the substrate in its vicinity.[23] The film surface remains smooth for any h value in the neutral region centered at $\gamma_{sn} \approx (38.2 \pm 0.8)$ mJ/m^2 ($\theta_w \approx 70.6° \pm 1.5°$), the average value from 8 different samples of all three molecular masses. The results match well with the neutral surface energy value of 38.6 mJ/m^2 estimated by Peters et al.[27] They arrived at the smooth neutral morphology at a constant thickness by casting films on painstakingly prepared individual test substrates where the interfacial energy of each substrate is tuned by grafting different composition random copolymer (PS-r-PMMA) brushes. The morphology shown in Figure 2 is common to all three M values and film thicknesses from (1.5 to 5) L_o and demonstrates how the h and γ_s dependence of the block copolymer morphology can be quickly mapped with combinatorial methods.

After the block copolymer library has been formed it can be characterized with higher resolution to investigate more refined features of this type of pattern formation. If higher magnification micrographs are acquired along a constant γ_s track, the familiar progression from smooth surface to islands to co-continuous to holes back to a smooth surface as a function of h is found.[3,4,19–21] Likewise, if a series of micrographs are obtained from a constant h path, the morphology is observed to change from symmetric to anti-symmetric with the nature of the surface patterns formed depending on h.[14] An example of this morphology change is shown in Figure 3 where AFM images of an $M = 51$k block copolymer film acquired at $h \approx 71$ nm (2.37 L_o) are presented. The images were obtained in tapping mode and have a common height scale (full range 50 nm) where the brighter color indicates tall features and the dark color indicates holes on the film surface. The labels in Figure 3 show the difference, $\Delta\gamma$, in the surface energy of each micrograph location, γ_s, from the neutral point, γ_{sn}, defined as

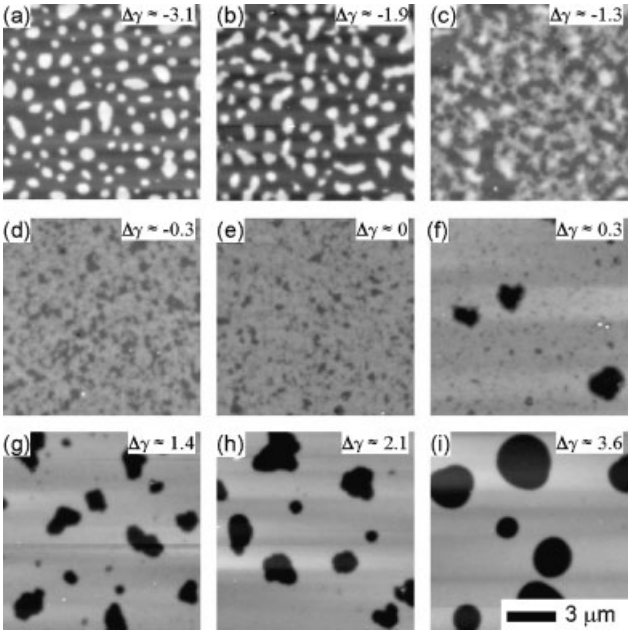

Figure 3. AFM images obtained from a constant film thickness ($h \approx 71$ nm) showing the inversion from island to hole morphology as a function of surface energy. The images have a common height scale (50 nm) and brighter features are islands and darker features are holes. The $\Delta\gamma$ labels indicate the difference between the substrate surface energy of the image location and the substrate surface energy at the center of the neutral region.

$\Delta\gamma = \gamma_s - \gamma_{sn}$ such that negative values of $\Delta\gamma$ correspond to lower values of γ_s. For $h = 71$ nm, the surface morphology is expected to be islands for the symmetric energy conditions ($\Delta\gamma < 0$ for the block copolymer used here) and holes for the anti-symmetric state ($\Delta\gamma > 0$) with a smooth surface in between ($\Delta\gamma \approx 0$, i.e. at γ_{sn}). This expectation is confirmed in Figure 3 where islands are found in the symmetric case (Figure 3a), holes are found in the anti-symmetric case (Figure 3i), and a relatively smooth region is found in between (Figure 3e).

Further examination of Figure 3 reveals that the degree of formation of the island and hole features is dependent on $\Delta\gamma$, an observation made significantly easier by using the combinatorial gradient technique employed here. For small values of $\Delta\gamma$, the affinity of one block for the surface relative to the other is weak and the surface features are small and not well defined. As the magnitude of $\Delta\gamma$ increases, the affinity to the surface of one block becomes stronger and the formation of lamellae parallel to the substrate and subsequent surface pattern formation is enhanced. This behavior is observed for all three molecular masses and for all morphologies associated with changing h. Notably a change of M affected the ''width'' of the neutral region, ω, such that for higher M the value of $\Delta\gamma$ for complete pattern formation increased. To quantify this behavior, the AFM micrographs were digitally analyzed to determine the average feature (hole or island) size, λ, in each image.

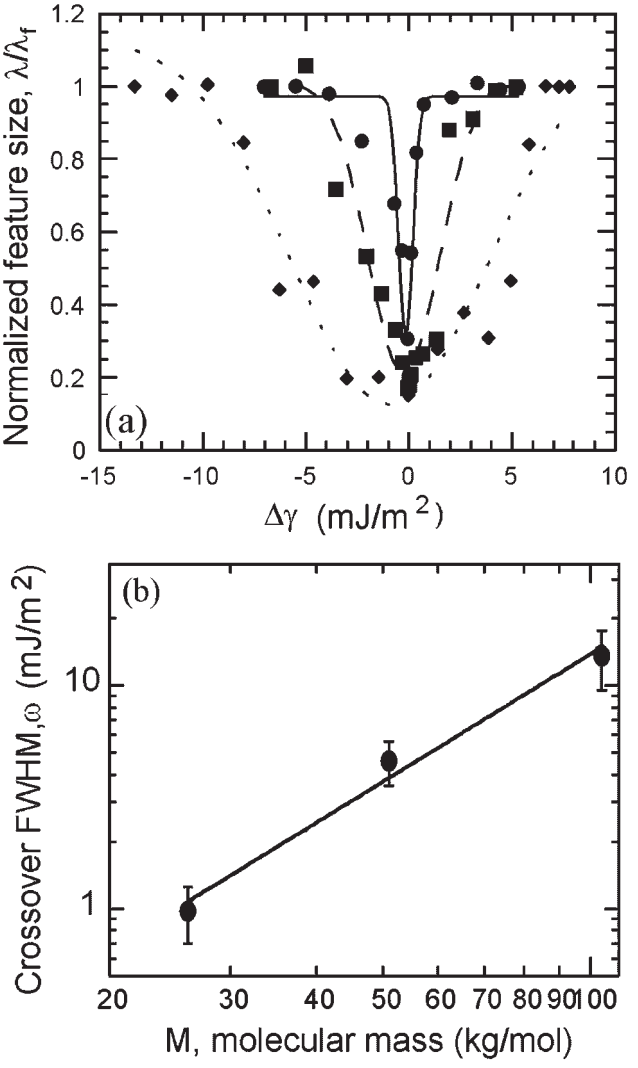

Figure 4. (a) Plot of the normalized feature size versus $\Delta\gamma$ for $M = 26$k (solid line), 51k (dashed line) and 104k (dotted line) block copolymers showing how the width of the neutral region changes as a function of molecular mass. Lines are least square fits of an inverted Gaussian to the data. (b) Plot of FWHM (ω) of Gaussian fit curves in Figure 4a as a function of $M(\omega \propto M^{1.9})$. The error bars in the figure denote the standard uncertainties from the Gaussian fits.

These values were normalized by the size of the features at large $\Delta\gamma$, λ_f, and plotted as a function of $\Delta\gamma$ as shown in Figure 4a. (The normalization of the feature size by λ_f was performed to account for the large differences in size between the holes and islands formed.) Figure 4a demonstrates that the $M = 26$k sample has a much narrower neutral region relative to the higher M samples. An inverted Gaussian function was least-squares fit to the data (lines in Figure 4a) and a full width at half peak maximum ($\omega = $FWHM) value is obtained (given in Table 1) as a measure of the magnitude of $\Delta\gamma$ for full feature formation. These ω values indicate that M has a significant effect on the lamellae formation of the block copolymers near the neutral

point $\gamma_s \approx \gamma_{sn}$. A plot of the ω vs M in Figure 4b yields an apparent power law dependence of $\omega \propto M^{1.9}$, although caution must be exercised due to the limited number and range of M values.

In our previous papers,[3,4] we have noted that the characteristic in-plane dimension, λ_p, of the surface block copolymer patterns generally scales with M as $\lambda_p \propto M^{-1.65}$. This effect was attributed to the increasing energetic cost of deforming the outer block copolymer surface layer arising from the theoretically expected increase in bending and compressional layer elasticity with M.[3,4] In the present measurements, however, it is not evident that the elasticity of the outer layer is the controlling factor for the scale of pattern formation. The crossover between the symmetric and the anti-symmetric morphologies across the neutral region ω must involve *all* of the lamellae layers. If the elasticity of the film as a whole were important, then we would expect ω to depend on film thickness since the film's elastic deformation energy should depend on the number of layers. We do not observe such an effect. Moreover, an elasticity effect of this kind would lead us to expect the width of the neutral region, ω, to depend on the magnitude of the surface energy gradient. Preliminary measurements with a substantially lower energy gradient (the gradient in Figure 2 is nearly a factor of two lower than in Figure 4 for the 51k polymer) indicate that ω does not depend on the surface energy gradient to within experimental uncertainty.[d] This seems to suggest a thermodynamic explanation of our observations.

It is clear that further measurements are required to fully explain the observations of a molecular-weight-dependant neutral zone revealed by our combinatorial measurements. Notably, this effect would have been difficult to detect in discrete measurements of films of fixed thickness due to the experimental difficulty in creating a large number of substrates with a systematic and precisely controlled variations in surface energy and film thickness. The gradients not only elucidate novel features of surface pattern formation, but also provide an unambiguous and convenient method for identifying conditions for morphological crossover in a self-reporting fashion.

Received: October 24, 2002
Revised: November 29, 2002
Accepted: December 4, 2002

[1] T. P. Russell, *Science* **2002**, *297*, 964.
[2] T. P. Russell, A. Menelle, S. H. Anastasiadis, S. K. Satija, C. F. Majkrzak, *Macromolecules* **1991**, *24*, 6263.
[3] A. P. Smith, J. F. Douglas, J. C. Meredith, E. J. Amis, A. Karim, *J. Polym. Sci., Part B: Polym. Phys.* **2001**, *39*, 2141.
[4] A. P. Smith, J. F. Douglas, J. C. Meredith, E. J. Amis, A. Karim, *Phys. Rev. Let.* **2001**, 8701.
[5] P. Mansky, O. K. C. Tsui, T. P. Russell, Y. Gallot, *Macromolecules* **1999**, *32*, 4832.
[6] T. P. Russell, R. P. Hjelm, P. A. Seeger, *Macromolecules* **1990**, *23*, 890.
[7] K. Tanaka, A. Takahara, T. Kajiyama, *Macromolecules* **1997**, *30*, 6626.
[8] A. M. Mayes, T. P. Russell, V. R. Deline, S. K. Satija, C. F. Majkrzak, *Macromolecules* **1994**, *27*, 7447.
[9] T. Xu, H. C. Kim, J. DeRouchey, C. Seney, C. Levesque, P. Martin, C. M. Stafford, T. P. Russell, *Polymer* **2001**, *42*, 9091.
[10] O. K. C. Tsui, T. P. Russell, C. J. Hawker, *Macromolecules* **2001**, *34*, 5535.
[11] G. Reiter, G. Castelein, P. Hoerner, G. Riess, A. Blumen, J. U. Sommer, *Phys. Rev. Lett.* **1999**, *83*, 3844.
[12] G. J. Kellogg, D. G. Walton, A. M. Mayes, P. Lambooy, T. P. Russell, P. D. Gallagher, S. K. Satija, *Phys. Rev. Lett.* **1996**, *76*, 2503.
[13] P. Mansky, T. P. Russell, C. J. Hawker, J. Mays, D. C. Cook, S. K. Satija, *Phys. Rev. Lett.* **1997**, *79*, 237.
[14] P. Mansky, T. P. Russell, C. J. Hawker, M. Pitsikalis, J. Mays, *Macromolecules* **1997**, *30*, 6810.
[15] P. Mansky, Y. Liu, E. Huang, T. P. Russell, C. J. Hawker, *Science* **1997**, *275*, 1458.
[16] F. S. Bates, G. H. Frederickson, *Annu. Rev. Phys. Chem.* **1990**, *41*, 525.
[17] P. F. Green, T. M. Christensen, T. P. Russell, R. Jérôme, *Macromolecules* **1989**, *22*, 2189.
[18] S. H. Anastasiadis, T. P. Russell, S. K. Satija, C. F. Majkrzak, *J. Chem. Phys.* **1990**, *92*, 5677.
[19] D. Ausserre, D. Chatenay, G. Coulon, B. Collin, *J. Phys. France* **1990**, *51*, 2571.
[20] G. Coulon, D. Ausserre, T. P. Russell, *J. Phys. (Paris)* **1990**, *51*, 777.
[21] G. Coulon, B. Collin, D. Ausserre, D. Chatenay, T. P. Russell, *J. Phys. (Paris)* **1990**, *51*, 2801.
[22] A. M. Mayes, T. P. Russell, P. Bassereau, S. M. Baker, G. S. Smith, *Macromolecules* **1994**, *27*, 749.
[23] E. Huang, T. P. Russell, C. Harrison, P. M. Chaikin, R. A. Register, C. J. Hawker, J. Mays, *Macromolecules* **1998**, *31*, 7641.
[24] E. Huang, L. Rockford, T. P. Russell, C. J. Hawker, *Nature* **1998**, *395*, 757.
[25] E. Huang, S. Pruzinsky, T. P. Russell, J. Mays, C. J. Hawker, *Macromolecules* **1999**, *32*, 5299.
[26] R. D. Peters, X. M. Yang, T. K. Kim, B. H. Sohn, P. F. Nealey, *Langmuir* **2000**, *16*, 4625.
[27] R. D. Peters, X. M. Yang, T. K. Kim, P. F. Nealey, *Langmuir* **2000**, *16*, 9620.
[28] T. K. Kim, X. M. Yang, R. D. Peters, B. H. Sohn, P. F. Nealey, *J. Phys. Chem. B* **2000**, *104*, 7403.
[29] S. V. Roberson, A. J. Fahey, A. Sehgal, A. Karim, *Appl. Surf. Sci.* **2002**, *200*, 150.
[30] L. A. Girifalco, R. J. Good, *J. Phys. Chem.* **1957**, *61*, 904.
[31] L. A. Girifalco, R. J. Good, *J. Phys. Chem.* **1960**, *64*, 561.
[32] J. Genzer, E. J. Kramer, *Phys. Rev. Lett.* **1997**, *78*, 4946.
[33] J. C. Meredith, A. P. Smith, A. Karim, E. J. Amis, *Macromolecules* **2000**, *33*, 9747.

[d] A detailed analysis and discussion will be presented in a future publication.